Volume 9, Number 11
1009-1963/2000/09(11)/0855-06
CHINESE PHYSICS
November, 2000
© 2000 Chin. Phys. Soc.

# CONSTRUCTION OF AN OPTICAL TWEEZERS —CALCULATION AND EXPERIMENTS

Sun Wei(孙 巍) and Wang Yi-qiu(王义遒)
*Department of Electronics, Peking University, Beijing* 100871, *China*
Gao Chong-ming(高崇明)
*College of Life Science, Peking University, Beijing* 100871, *China*

(Received 3 April 2000; revised manuscript received 7 June 2000)

We report the construction of an optical tweezers system and the results of the trapping and the moving of living algal cells. Experimental study on trapping polystyrene spheres demonstrates the effects of the system parameters on the trap. The trapping forces on dielectric spheres are calculated using Ashkin's ray-optics model. The result shows that an objective with higher numerical aperture can build a more stable trap along axial direction than an objective with lower numerical aperture, though their transverse trapping forces are on the same order.

**Keywords:** optical tweezers, light force, cell biology
**PACC:** 8780, 4279

## I. INTRODUCTION

The single-beam optical trap, or optical tweezers, is a novel technique that applies laser in cell biology. The tweezers consist of a highly focused laser beam, usually by the objective of a microscope, which at the same time is used to observe the manipulated objects. In the presence of such a beam, a dielectric sphere is polarized by electric field, and due to the high intensity gradient of the light field it is drawn to the beam focus and then trapped there. In 1986, Ashkin and his cooperators constructed the first optical tweezers,[1] and proved that it could also trap biological objects, such as living cells or organelles, without damage.[2] Since then, more and more interests appeared, and important works have been done in this field.[3]−[8] Optical tweezers have now become widely using tool in cell biology. In China, to our knowledge, a group at University of Science and Technology of China first began to explore this technique and has trapped biological cells successfully.[9] Recently, a group at the Institute of Physics in Chinese Academy of Science has been engaged in this field. They studied the transverse stability of trapping force in optical tweezers.[10]

For constructing optical tweezers for some special purpose we need to calculate the force necessary for trapping and manipulating the objects interested. There are two methods of calculating the tapping forces: ray-optics model and electromagnetic-field model. The calculation of electromagnetic-field model is cumbersome[11]. When the diameter of the tapped sphere $d \gg \lambda$ (where $\lambda$ is the wavelength of the laser), results from the ray-optics model are in good agreement with those from the electromagnetic-field model. We use Ashkin's ray-optics model to calculate the forces[12].

In this paper, we describe the calculation method and results, the setup and the experimental results of our optical tweezers system. We have successfully trapped and moved living algal cells, 1$\mu$m and 0.5$\mu$m polystyrene spheres. With polystyrene spheres, we have also studied the performance of the tweezers system, and the effects of variations of some parameters, such as the numerical aperture of the objective and the diameter of the trapped spheres.

## II. CALCULATION

In ray-optics model, the light beam is decomposed into individual rays. Trapping forces of tweezers are results from the momentum change of input photons due to the reflection and refraction of the incident rays by dielectric spheres. So the total force exerted on the sphere is the sum of contributions of individual rays in the beam. According to Refs.[12,13], the net force $f$ on the sphere can be broken into two components:

$$\boldsymbol{f} = \boldsymbol{f}_{\rm s} + \boldsymbol{f}_{\rm g} = \boldsymbol{Q}_{\rm total}\frac{n_1 P}{c} = (\boldsymbol{Q}_{\rm total\,s} + \boldsymbol{Q}_{\rm total\,g})\frac{n_1 P}{c}$$
$$= \frac{n_1 P}{c\pi a_{\rm max}^2}\sum_{\rm all\ rays}(Q_{\rm s} + Q_{\rm g})\cdot\Delta S, \quad (1)$$

$$Q_{\rm total} = Q_{\rm total\,g} + Q_{\rm total\,s}, \quad (2)$$

where $f_{\rm s}=\sum\limits_{\text{all rays}}\boldsymbol{F}_{\rm s}$ is the scattering force component and $f_{\rm g}=\sum\limits_{\text{all rays}}\boldsymbol{F}_{\rm g}$ is the gradient force component of a beam, and $\boldsymbol{F}_{\rm s}$ and $\boldsymbol{F}_{\rm g}$ are the corresponding force components for a single ray. $\pi a_{\max}^2$ is the cross-section of the beam with radius $a_{\max}$, $\Delta S$ is the cross-section of a single ray and $n_1P/c$ is the incident momentum per second in a medium of index of refraction $n_1$.

$$\begin{aligned}Q_{\rm s}=&\frac{1}{2}\left\{1+R_{\hat{s}}\cos 2\theta\right.\\&\left.-\frac{T_{\hat{s}}^2[\cos(2\theta-2r)+R_{\hat{s}}\cos 2\theta]}{1+R_{\hat{s}}^2+2R_{\hat{s}}\cos 2r}\right\}\\&+\frac{1}{2}\left\{1+R_{\hat{p}}\cos 2\theta\right.\\&\left.-\frac{T_{\hat{p}}^2[\cos(2\theta-2r)+R_{\hat{p}}\cos 2\theta]}{1+R_{\hat{p}}^2+2R_{\hat{p}}\cos 2r}\right\},\end{aligned}\tag{3}$$

$$\begin{aligned}Q_{\rm g}=&\frac{1}{2}\left\{R_{\hat{s}}\sin 2\theta\right.\\&\left.-\frac{T_{\hat{s}}^2[\sin(2\theta-2r)+R_{\hat{s}}\sin 2\theta]}{1+R_{\hat{s}}^2+2R_{\hat{s}}\cos 2r}\right\}\\&+\frac{1}{2}\left\{R_{\hat{p}}\sin 2\theta\right.\\&\left.-\frac{T_{\hat{p}}^2[\sin(2\theta-2r)+R_{\hat{p}}\sin 2\theta]}{1+R_{\hat{p}}^2+2R_{\hat{p}}\cos 2r}\right\},\end{aligned}\tag{4}$$

where $R_{\hat{s}}$ and $T_{\hat{s}}$ are the Fresnel reflection and transmission coefficients when polarization is along $\hat{s}$ direction, and $R_{\hat{p}}$ and $T_{\hat{p}}$ are those when polarization direction is along $\hat{p}$. The notation is the same as in Ref.[12] (see Figs.1 and 2 cited from [12]).

We consider two situations:

(1) Trap focus along $Z$ axis of the sphere

First, we consider the case where the trap focus $f$ is located along $Z$-axis at a distance $S$ above the sphere center $O$, as shown in Fig.1. The objective has radius $a_{\max}$ and focal length $l$, and the radius of the sphere is taken as 1. Consider an arbitrary incident ray that hits the objective at radius $\alpha$ and angle $\beta$ in $WZ$ plane. The ray and the beam axis make an angle $\phi$ ($\phi_{\max}$ is determined by numerical aperture N.A.$=n_1\sin\phi_{\max}$). $\theta$ and $r$ are the angles of incidence and refraction, respectively.

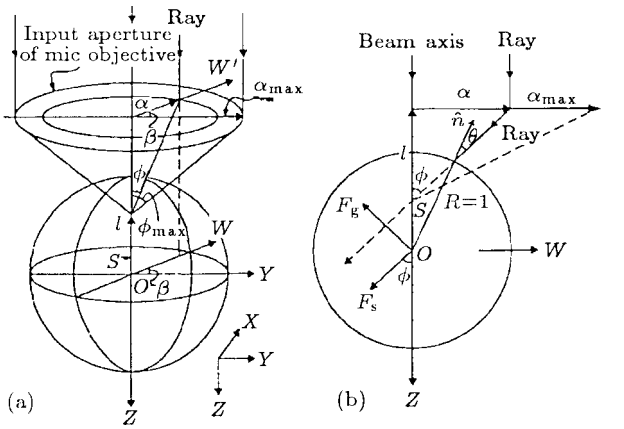



**Fig.1.** (a) Single-beam gradient force trap in the ray optics model with beam focus $f$ located along the $Z$-axis of the sphere. (b) Geometry of an incident ray giving rise to gradient and scattering force contributions $F_{\rm g}$ and $F_{\rm s}$.

Due to axial symmetry, the resultant $Q_{\text{total s}}$ and $Q_{\text{total g}}$ point in the direction of $+\hat{z}$ or $-\hat{z}$.

$$\begin{aligned}Q_{\text{total s}}&=\frac{2\pi\int_{a=0}^{a_{\max}}Q_{{\rm s}z}a{\rm d}a}{\pi a_{\max}^2}\\&=\frac{2}{a_{\max}^2}\int_{a=0}^{a_{\max}}Q_{\rm s}\cos\phi a{\rm d}a,\end{aligned}\tag{5}$$

$$\begin{aligned}Q_{\text{total g}}&=\frac{2\pi\int_{q=0}^{a_{\max}}Q_{{\rm g}\,z}a{\rm d}a}{\pi a_{\max}^2}\\&=\frac{2}{a_{\max}}\int_{a=0}^{a_{\max}}(-Q_{\rm g}\cos\phi)a{\rm d}a,\end{aligned}\tag{6}$$

where values of $\theta, r, \phi$ can be given by $\tan\phi=\dfrac{a}{l}$, $\sin\theta=S\sin\phi$, and $n_1\sin\theta=n\sin r$.

(2) Trap focus along $Y$ axis of the sphere

We next examine the trapping force when focus $f$ is located along the $Y$-axis of the sphere at a distance of $S'$ from $O$, as shown in Fig.2. An arbitrary incident ray hits the objective at $V$ in $AWW'f$ plane, and makes an angle $\alpha$ with line $fW'$. Directions of scattering force component $F_{\rm s}$ and gradient force component $F_{\rm g}$ of the incident ray run parallel with plane $fVO$, which contains the incident ray and the normal $\hat{n}$. The incident ray and $Y$-axis make an angle $\gamma$. Values of $\theta, r, \alpha$ and $\gamma$ can be given by $\tan\alpha=l/a$, $\sin\theta=S'\sin\gamma$, and $\cos\gamma=\cos\alpha\cos\beta$. We have

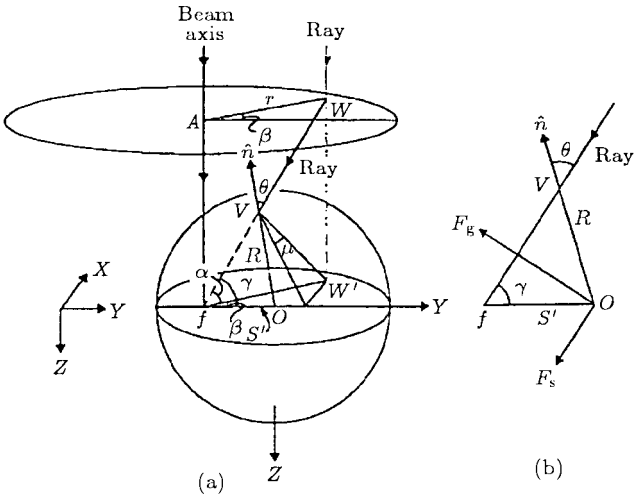



**Fig.2.** (a) Trap geometry with the beam focus $f$ located transversely along the $Y$-axis at a distance $S'$ from the origin. (b) Geometry of the plane of incidence, showing the directions of the gradient and scattering forces $F$ and $F_s$ for the input ray.

$$Q_{\text{total}sz} = \frac{\int_{\beta=0}^{2\pi}\int_{a=0}^{a_{\max}} Q_{sz}a\,da\,d\beta}{\pi a_{\max}^2} = \frac{2}{\pi a_{\max}^2}\int_{\beta=0}^{\pi}\int_{a=0}^{a_{\max}}(Q_s\sin\alpha)a\,da\,d\beta, \quad (7)$$

$$Q_{\text{total}\,gz} = \frac{\int_{\beta=0}^{2\pi}\int_{a=0}^{a_{\max}} Q_{gz}a\,da\,d\beta}{\pi a_{\max}^2} = \frac{2}{\pi a_{\max}^2}\int_{\beta=0}^{\pi}\int_{a=0}^{a_{\max}} Q_g\left(-\frac{\sin\alpha}{\tan\gamma}\right)a\,da\,d\beta, \quad (8)$$

$$Q_{\text{total}\,sy} = \frac{\int_{\beta=0}^{2\pi}\int_{a=0}^{a_{\max}} Q_{sy}a\,da\,d\beta}{\pi a_{\max}^2} = \frac{2}{\pi a_{\max}^2}\int_{\beta=0}^{\pi}\int_{a=0}^{a_{\max}} Q_s(-\cos\alpha\cos\beta)a\,da\,d\beta, \quad (9)$$

$$Q_{\text{total}\,gy} = \frac{\int_{\beta=0}^{2\pi}\int_{a=0}^{a_{\max}} Q_{gy}a\,da\,d\beta}{\pi a_{\max}^2} = \frac{2}{\pi a_{\max}^2}\int_{\beta=0}^{\pi}\int_{a=0}^{a_{\max}} Q_g(-\sin\gamma)a\,da\,d\beta. \quad (10)$$

## III. CALCULATED RESULT

We develop a FORTRAN program to calculate the integrals in expressions (5)–(10) and plot the results in Figs.3–8 using software Origin 5.0.

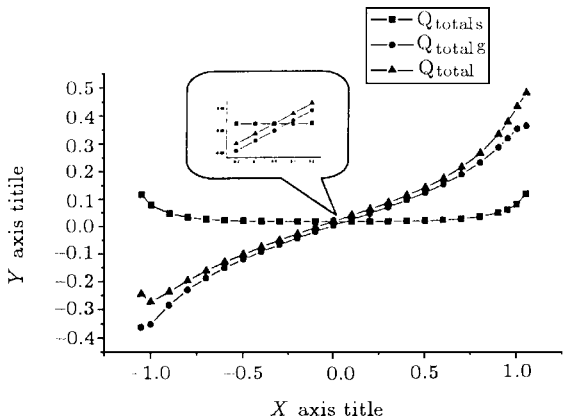



**Fig.3.** Values of scattering force, gradient force and total force $Q_{\text{totals}}$ $Q_{\text{total}\,g}$ and $Q_{\text{total}}$ exerted on a polystyrene sphere in water by a trap, which is focused along the $Z$-axis by a N.A.=1.25 objective. The radius of the sphere is 1.

First, we take a N.A.=1.25 oil immersion objective for example. We know that directions of the scattering force, gradient force and total force are all parallel with $+Z$-axis when the trap focus $f$ is located on $Z$-axis. Magnitudes of these forces are plotted in Fig.3, in which we can find that the gradient force always points to the trap focus $f$ but the scattering force always points to $+\hat{z}$ direction. We can also find that the absolute value of the gradient force exceeds the scattering force in region of $|S| > 0.07$, this means the trap is stable. The stable equilibrium point $S_e$ of the trap is located at $S \approx 0.07$, where the total force is zero.

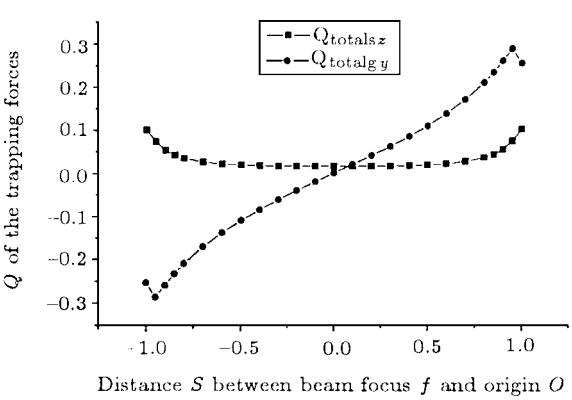



**Fig.4.** Values of scattering force $Q_{\text{totals}}$ and gradient force $Q_{\text{total}\,g}$ exerted on a polystyrene sphere in water by a trap, which is focused along the $Y$-axis by a N.A.=1.25 objective.

Figure 4 shows similar results when the trap focus $f$ is located on $Y$-axis. Although the direction of the gradient force is parallel with $Y$-axis, it always points to the focus $f$ and the scattering force always points to $+\hat{z}$ direction still.

Figures 5 and 6 are the results of a N.A.=0.65 objective. There is not much difference between Figs.4 and 6, when the focus $f$ is located on $Y$-axis, but the forces change dramatically when focus $f$ is located on $Z$-axis, as shown in Fig.5. The gradient force is obviously smaller than that in Fig.3 and stable equilibrium point $S_e$ is located at $S \approx 0.69$, where the sphere can escape from the trap more easily if perturbed. All this means the trap is weaker along $Z$-axis when using a lower numerical aperture objective, though the tranverse trapping force does not change much.

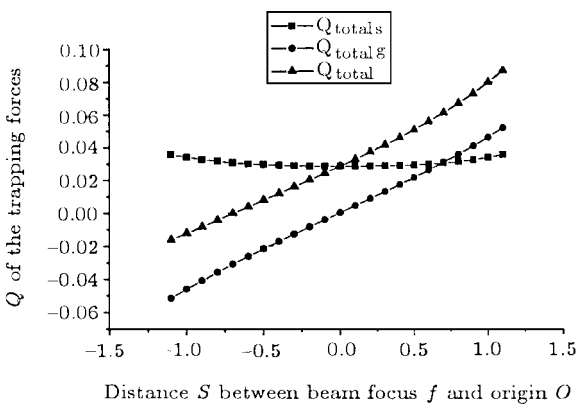



**Fig.5.** Values of scattering force, gradient force and total force $Q_{\text{totals}}$ $Q_{\text{totalg}}$ and $Q_{\text{total}}$ exerted on a polystyrene sphere in water by a trap, which is focused along the $Z$-axis by a N.A.=0.6 objective.

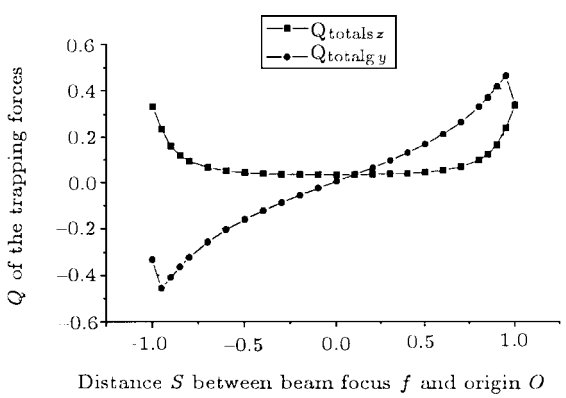



**Fig.6.** Values of scattering force $Q_{\text{totals}}$ and gradient force $Q_{\text{totalg}}$ exerted on a polystyrene sphere in water by a trap, which is focused along the $Y$-axis by a N.A.=0.6 objective.

Effects of the refractive index of the sphere are also studied. Figures 7 and 8 show values of the trapping forces acting on a sphere of refractive index $n$ in a trap focused by a N.A.=1.25 objective. We can see the maximum magnitude of the total force occurs when $n$ equals to 1.65 and a quite good performance can be got over the range $n = 1.5$ to $n = 2.0$, which covers most biological samples.

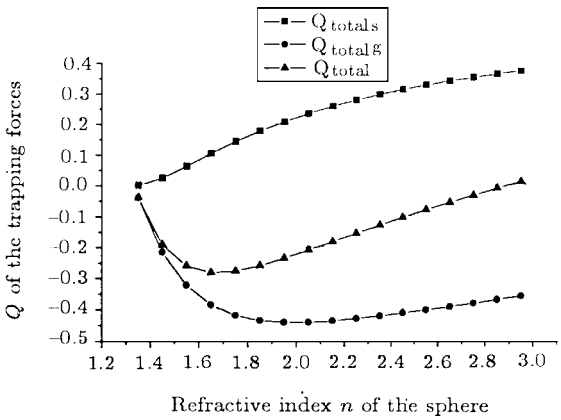



**Fig.7.** Values of scattering force, gradient force and total force $Q_{\text{totals}}$ $Q_{\text{totalg}}$ and $Q_{\text{total}}$ exerted on a sphere of refractive index $n$ in water by a trap, which is focused along the $Z$-axis at position $s$=1 by a N.A.=1.25 objective.

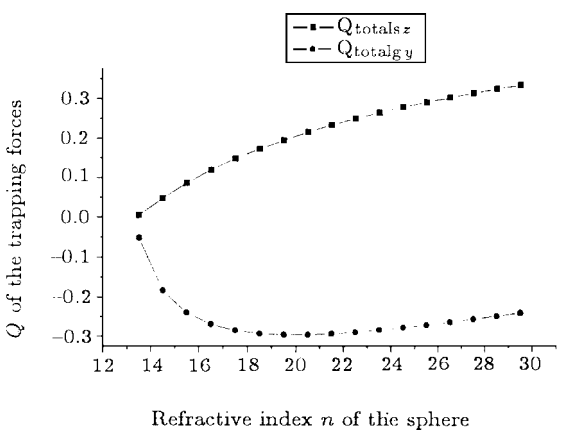



**Fig.8.** Values of scattering force $Q_{\text{totals}}$ and gradient force $Q_{\text{totalg}}$ exerted on a sphere of refractive index $n$ in water by a trap, which is focused along the $Y$-axis at position $s'$=1 by a N.A.=1.25 objective.

Our results also show that the gradient force is independent of sphere radius $r$ in the regime in which $r \gg$ laser wavelength $\lambda$. Since the force varies as $r^3$ in the Rayleigh regime in which $r \ll \lambda$,[1] we can expect the force varies between $r^0$ and $r^3$ in the intermediate regime in which $r \approx \lambda$.

We also neglect effects of polarization direction on the trapping forces in the preceding calculation. Experiment of Wright and his co-workers showed that

when the gradient force is parallel with the polarization direction, it is a little bit larger than that when the force is perpendicular to the polarization direction while the linear polarization laser is used.[14]

## IV.SETUP OF THE SYSTEM

The preceding calculation gives us a clear guide for constructing a tweezers system. As the widely used method, we introduce the output of laser to an objective lens of a microscope to get a highly focused beam and the microscope is used as the observing tool at the same time. In the preceding section, we know that an important parameter that affects the trapping force is the numerical aperture of the objective. This is important for choosing the microscope. We use in our experiment a fluorescent microscope, which has a fluorescent port that can let the laser beam in.

We choose an 850nm-wavelength diode laser to avoid damage of biological samples. In the preceding section, we have known that whether the trap can work is independent of the laser power, though the gradient force and the scattering force both increase with the increase of the laser power. When a spherical bead is moving in the liquid, the viscous force exerted on the sphere takes the form of the Stokes drag force:

$$F_{\mathrm{d}} = 6\pi\eta r v_{\mathrm{c}} \tag{11}$$

where $\eta$ is the viscosity of the liquid, $r$ is the radius of the bead, and $v_{\mathrm{c}}$ is the velocity of the bead.[15] Thus, taking $\eta = 10^{-3}\,\mathrm{N/m^2}$, to drag the sphere with a diameter of $10\mu$m at $20\mu$m/s we need to overcome a drag force $F_{\mathrm{d}}$ of 2pN. We choose a 50mW nominated power laser to get at least 2mW power in the specimen plane and about 2.2pN transverse gradient force is obtained.

The diagram of the tweezers system is depicted in Fig.9. Since the cross-section of the diode laser output is an elliptical light spot, two prisms are used to compress it to an approximate circular spot on circular cross-section of the objective (using cylindrical lenses can produce more satisfactory result). Lenses $L_1$ and $L_2$ expand the beam diameter to the objective lens diameter of 6mm in order to get the largest intensity gradient within the limit of the numerical aperture of objective $L_{\mathrm{o}}$. Meanwhile, by adjusting the distance between $L_1$ and $L_2$, we can adjust the position of the trap focus along the beam axis. Mirrors $M_1$ and $M_2$ are used to manipulate the beam position. Adjusting the angles of the mirrors between lenses $L_1$ and $L_2$ can change the angle of the beam incident into the microscope, i.e. changing the trap position in specimen plane. From a simple geometry, we get an expression for the trap displacement $\Delta y$ in the specimen plane,

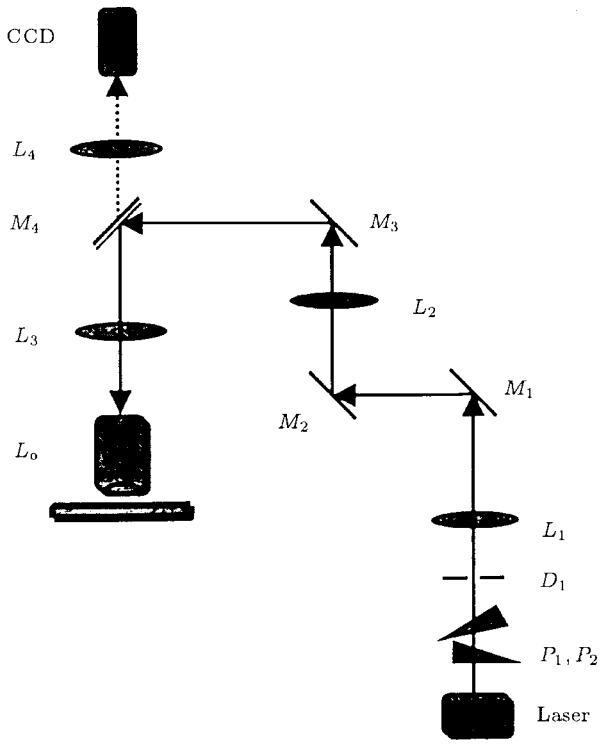



**Fig.9.** Schematic Diagram of the optical tweezers system: $P_1, P_2$: prisms; $D_1$: diaphragm; $L_1, L_2$: lenses for beam expanding; $M_1, M_2$: mirrors for beam steering; $M_3$: mirror; $M_4$: dichroic mirror; $L_3, L_4$: auxiliary lenses in the microscope.

$$\Delta y = \frac{f_{\mathrm{o}}}{f_2} \cdot s_1 \sin 2\theta_1, \tag{12}$$

where $f_{\mathrm{o}}$ and $f_2$ are the focal lengths of $L_{\mathrm{o}}$ and $L_2$ respectively, $\theta_1$ is the angle that $M_1$ turns, and $S_1$ is the distance between $M_1$ and the focal plane of $L_1$. From this expression, we know that we can get a more precise displacement of the trap by simply increasing $L_2$'s focal length $f_2$. There is a similar expression when the angle of $M_2$ changes. In our design we can get a precision displacement of the tweezers as small as 3.5 micrometers in the specimen plane.

$M_4$ is a dichroic mirror, and is specially designed for us to reflect the infrared light and lets visible light from illuminating source pass through.

Before we trap living cells, our test particles are polystyrene spheres with diameters of $1\mu$m and $0.5\mu$m and refractive index of 1.59.

## V. RESULT

Figure 10 shows some pictures of trapping and moving living algal cells with our tweezers system.

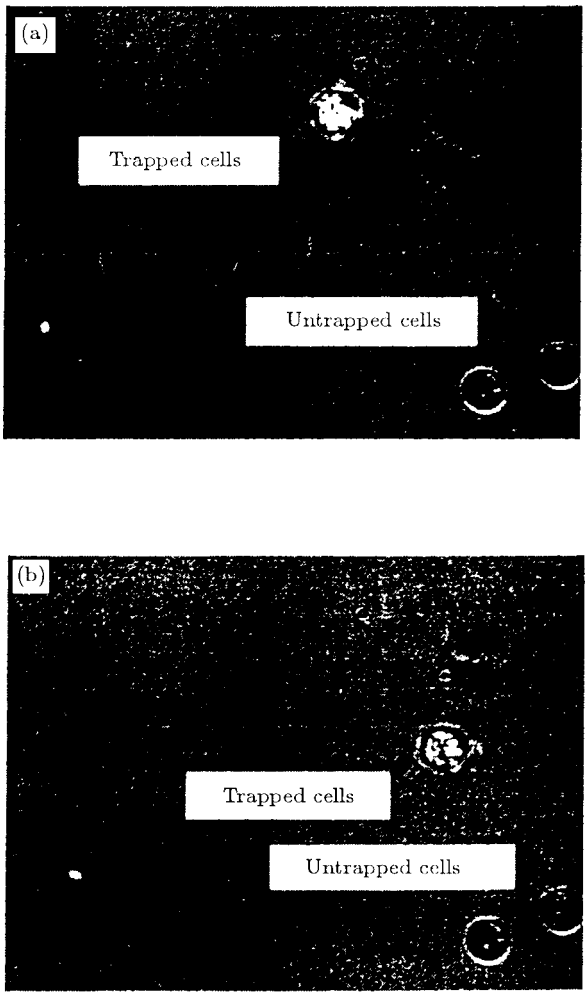



**Fig.10.** Images of demonstration of trapping and moving living algal cells with 40× N.A.=0.65 objective.

The size of each image is 100$\mu$m ×75$\mu$m, so we can see from the images that the size of the trapped cell is about 10$\mu$m and it is moved by 25$\mu$m. The trapped cell looks brighter than untrapped cells since it scatters some laser light. The diameter of the laser spot is about 2–3$\mu$m, which is very close to the diffraction-limited diameter 1.6$\mu$m.

Besides, we studied the effects of the parameters of the tweezers with polystyrene spheres. Experiments of trapping and moving two sizes of spheres are done with two types of objectives: 40× N.A.=0.65 objective and 100× N.A.=1.25 oil-immersion objective.

One experiment is to examine the minimum laser powers needed to trap two sizes of spheres with two objectives. Our result is as follows Table 1.

**Table 1**

| | objective 40× | objective 100× |
|---|---|---|
| Minimum power needed to trap a sphere with $d$=1$\mu$m | 0.03mW | 0.01mW |
| Minimum power needed to trap a sphere with $d$=0.5$\mu$m | 0.16mW | 0.06mW |

When trapping different sizes of spheres with one objective, the smaller sphere needs more power, which is consistent with our discussion that the gradient force varies between $r^0 \sim r^3$ in regime where $r \approx \lambda$. When trapping a spherical bead with different objectives, more power is required with 40× objective and we believe the reason is that its gradient force along $Z$-axis much smaller than the trap with 100× objective.

We also find that as many as 10 spherical beads can be trapped in the same spot after the waiting time of about 30 minutes.

We discover that we can only move the trapped bead by up to only 15–20 micrometers along $Z$-axis by moving the specimen plane, while there is almost no limit by moving the specimen plane along $X$-axis and $Y$-axis. This can be explained as a result of aberration.[12][10]

## REFERENCES

[1] A. Ashkin, J. M. Dziedzic, J. E. Bjorkholm, S. Chu, *Opt. Lett.*, **11**(1986),288.
[2] A. Ashkin, J. M. Dziedzic, *Science*, **235**(1987),1517.
[3] K. Sasaki, M. Koshioka, H. Misawa, *Japan. Jour. Appl. Phys.*, **30**(1991),907.
[4] T. T. Perkins, D. E. Smith, S. Chu, *Science*, **264**(1992), 819.
[5] K. Svoboda, C. F. Schmidt, B. J. Schnapp, S. M. Block, *Nature*, **365**(1993),721.
[6] K. Saito, Takaaki Aoki, Toshiaki Aoki, T. Yanagida, *Biophys. J.*, **66**(1994),768.
[7] K. Svoboda, S. M. Block, *Opt. Lett.*, **19**(1994),930.
[8] H. Liang, W. H. Wright, C. L. Rieder, E. D. Dalmon, G. Profeta, J. Andrews, Y. Liu, G. J. Sonek, M. W. Berns, *Exp. Cell Res.*, **213**(1994),308.
[9] Yin-mei Li, Xun-bin Wei, Tian Zhu, Run-long Lu, *Laser Biology*, **2**(1993),193(in Chinese).
[10] Xin-cheng Yao, Zhao-lin Li *et al.*, *Chin. Phys.*, **9**(2000),65.
[11] J. P. Barton, D. R. Alexander, S. A. Schaub, *J. Appl. Phys.*, **66**(1989),4594.
[12] Edited by M. P. Sheetz, Laser Tweezers in Cell Biology, Methods in Cell Biology Series, Vol.55(Academic Press, 1998).
[13] G. Roosen, *Can. J. Phys.*, **57**(1979),1260.
[14] W. H. Wright, G. J. Sonek, M. W. Berns, *Applied Optics*, **33**(1994),1735.
[15] H. Felgner, O. Muller, M. Schliwa, *Applied Optics*, **34**(1995),977.